CHAPTER IV

RESULTS AND DISCUSSION

Previously, many researchers attempted to develop and rectify the crucial issue on stability of capsinoids. One research group from Ajinomoto Co., Inc. observed the degradation of capsinoids and concluded that capsinoids was degraded through *p*-quinonemethide pathway and stabilization approach was also proposed.

They suggested that addition of a slightly excess amount of fatty acid coexisting with *p*-quinonemethide could convert *p*-quinonemethide to capsinoids in high yields. Unfortunately, the by-product decomposition, *p*-quinonemethide, sequentially and randomly reacted not only with fatty acid but also with hydroxyl group of phenol and produced undesired ester compounds then shifting toward to polymeric by-product. (Scheme 16)

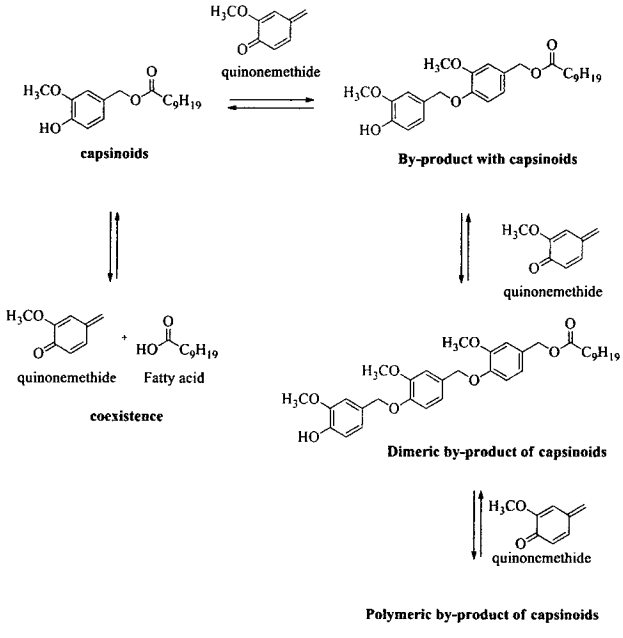

Scheme 16 Equilibrium state of quinonemethide, degradation by-product from capsinoids

To investigate how to better inhibit the *p*-quinonemethide degradation, capsinoid analogues were designed and synthesized by inversion of ester bond position while preserving H-bonding interaction between phenolic residue and receptor. To achieve this approach, capsinoid analogues (**4-7**) were synthesized *via* esterification between homovanillic acid (**14**) and fatty alcohol **12**, **13**, **17** and **18** using DCC, HOBt and DMAP as coupling agent. Moreover, the stability of capsinoid analogues (**4-7**) were conducted by quantitative analysis of residual of capsinoid analogues *via* HPLC technique compared with capsiate. Finally, their cytoxicity in Caco-2 cell were evaluated by MTT assays for observing cytoxicity of the novel capsinoid derivatives.

Synthesis of capsinoid analogue 4 and 5

The synthesis of capsinoid analogue **4** and **5** *via* esterification was consisting of two parts: carboxylic acid residue and alcohol segment (Scheme 17). Homovanillic acid was commercial available; however, alcohol segment must be synthesized and there were three approaches to prepare alcohol segment based on starting material; using bromoalcohol, bromoester and bromoacetic acid as starting material.

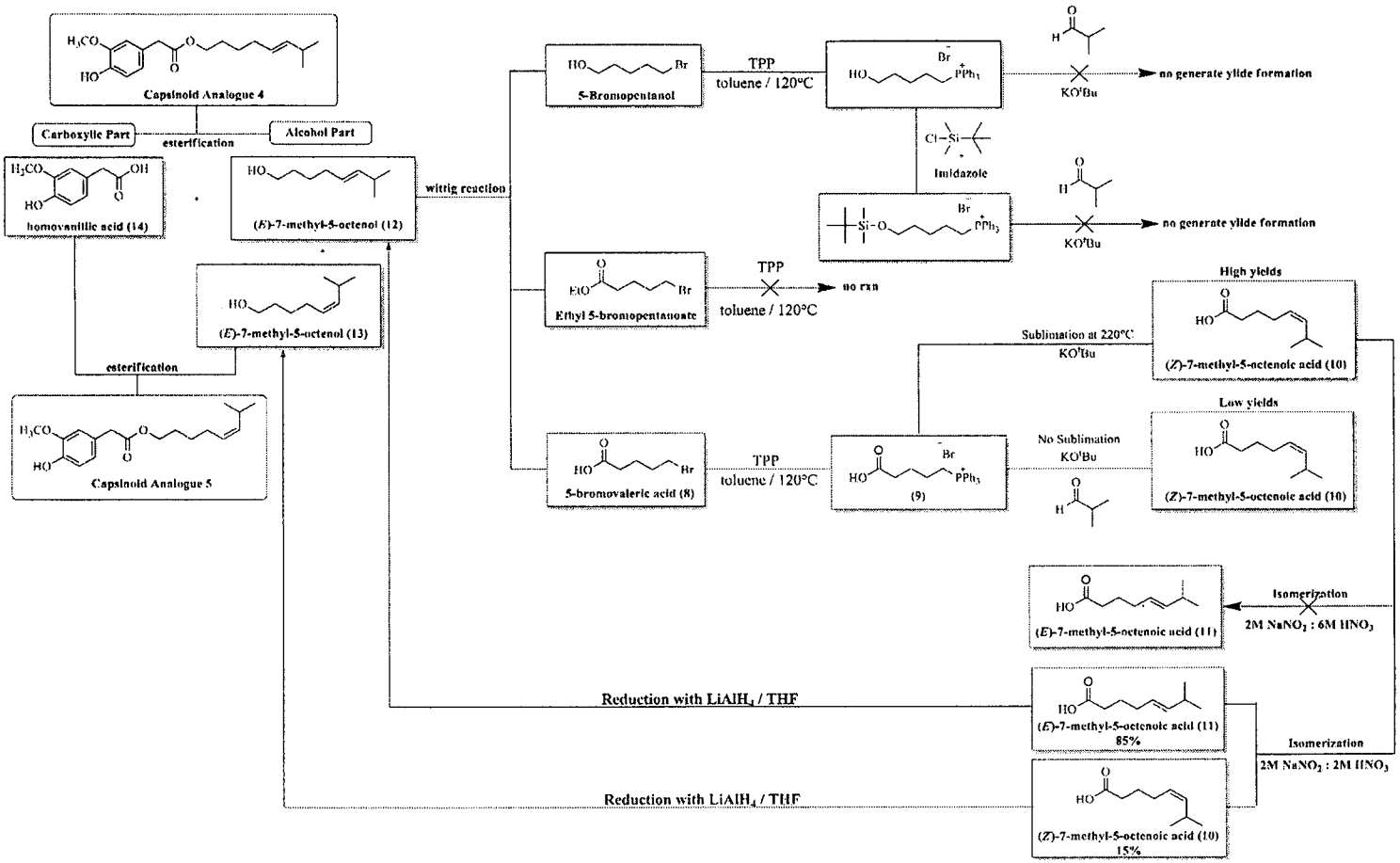

Scheme 17 The overview synthesis of capsinoid analogue 4 and 5

1. Synthesis of (*E/Z*)-7-methyl-5-octenol (12 and 13)

(*E/Z*)-7-Methyl-5-octenol (**12** and **13**) is an unsaturated C9 fatty alcohol (lipophilic carbon chain region). To synthesize the fatty alcohol chain, three different starting material was selected as follows; bromoalcohol, bromoester and bromoacetic acid.

First, 5-bromopentanol, a commercial available alcohol, was initially chose to react with TPP at elevated temperature and expected that TPP would selectively react with bromine to form triphenylphosphonium bromide salt; however, none of ylide formation did not observe. Additionally, protecting OH group of 5-bromopentanol with trimethylsilylchloride was performed and formation of desired bromide salt did not detect.

Second approach, ethyl-5-bromovalerate was selected as starting material. It was found that crude product from this reaction could not recrystallize in form of triphenylphosphonium bromide salt; consequently, impurity interfered during the ylide formation.

Final approach, 5-bromovaleric acid (**8**) and triphenyl phosphine was dissolved in toluene and then refluxed at 70 °C to generate a triphenylphosphonium salt (**9**), after reaction completed, the glassy mixture was triturated with CH_2Cl_2 and diethyl ether to give the clear crystal of desire product with 98% yields. In this step, the mechanism is conformable through S_N2 reaction. (Appendix B)

The identification structure of **9** was confirmed by ^1H NMR, the multiplet protons of aromatic on triphenyl group was appeared at 7.94-7.76 ppm (Figure 17).

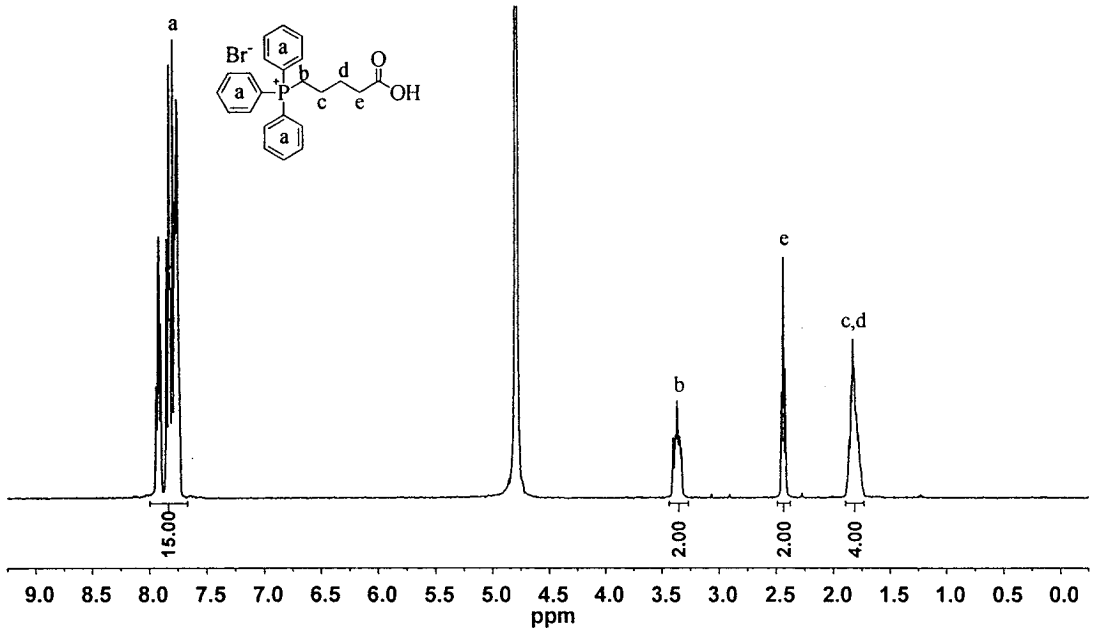

Figure 17 ^{1}H NMR Spectrum of (4-carboxybutyl)triphenylphosphonium bromide (9) δ 7.94-7.76 ppm verified aromatic protons of triphenyl group (m, aromatic-H, 15H) (D_2O)

After that, potassium *tert*-butoxide (KO^tBu) was used to deprotonate proton to generated phosphine ylide as Wittig reagent. Immediately, the ylide performed as a nucleophile and attacked to carbonyl carbon of isobutyraldehyde. The resulting was alkoxide oxygen attacked to the phosphorus in an intramolecular closure reaction *via* puckered transition state which irreversible and concerted. In the first place, [2+2] Cycloaddition forming a four-membered ring, generated an oxaphosphetane intermediate and the next, triphenylphosphine oxide was formed and produce (*Z*)-7-methyl-5-octenoic acid (**10**) (Appendix B). The structure of **10** was identified by ^{1}H NMR and the key signal was unsaturated protons at δ 5.29-5.12 ppm indication of olefinic proton (Figure 18).

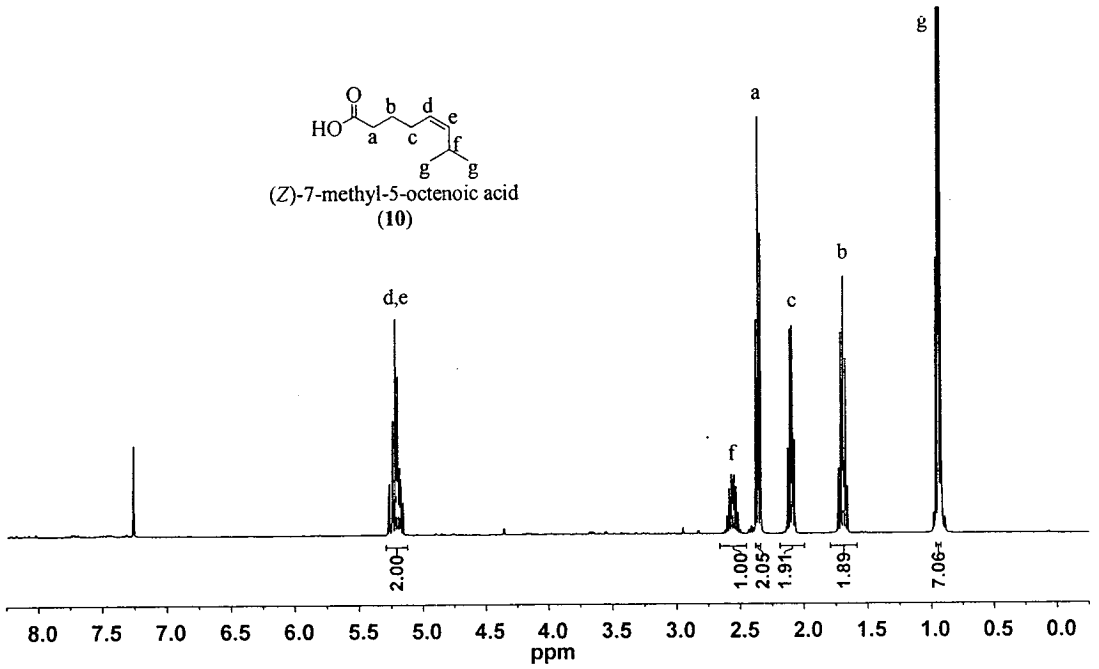

Figure 18 ^{1}H NMR Spectrum of *(Z)*-7-methyl-5-octenoic acid (10) identity signal of unsaturated protons at δ 5.29 – 5.12 ppm (m, CH=CH, 2H) ($CDCl_3$)

Then, (*Z*)-7-methyl-5-octenoic acid (**10**) was transformed to *E*-isomer by reacting with nitrous acid using sodium nitrite and nitric acid as reagent. In the presence of acidic conditions, nitrous acid turned into nitrosonium cation and acts as an electrophile to acquire electrophilic addition at alkene region. This initiated sp^2 carbon center changed from sp^2 to sp^3-hybridization. Consequently, elimination of nitrous acid was again converted sp^3 to sp^2-hybridization to afford a mixture of **11** and **10** (*E/Z* isomer = 85:15).

The structure of *(E/Z)*-7-methyl-5-octenoic acid (**11** and **10**) was verified by ^{1}H NMR, found that the chemical shift of proton on tertiary carbon was shift from 2.59-2.48 to 2.27-2.18 ppm owing to the anisotropic effect (Figure 19).

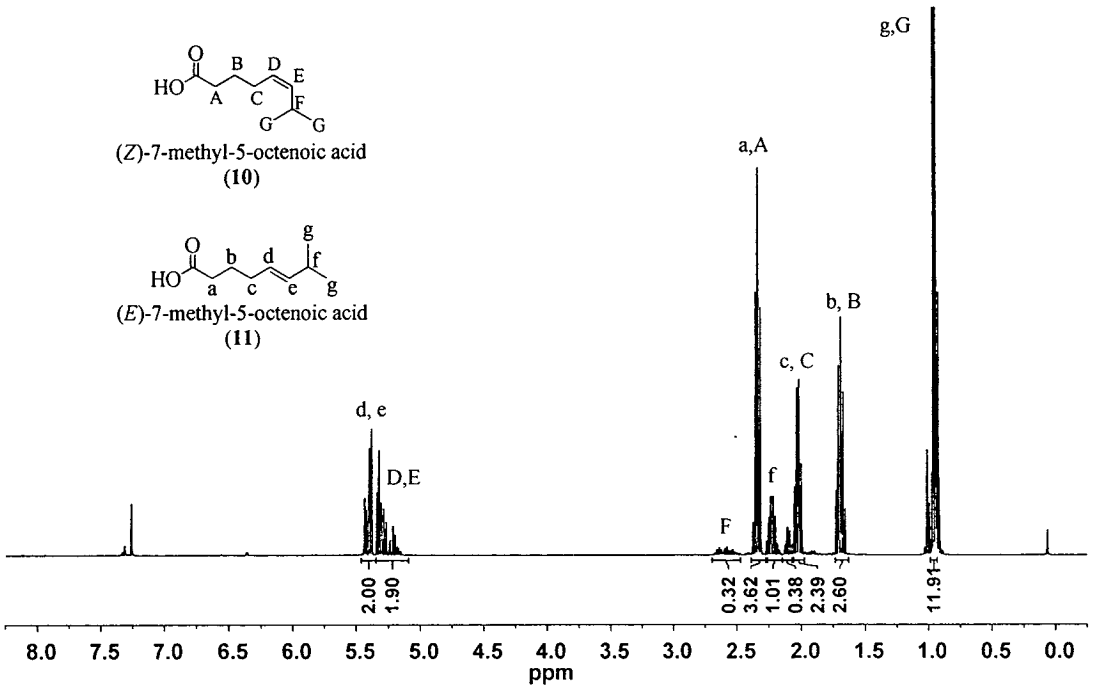

Figure 19 ^{1}H NMR Spectrum of mixture (*E*/Z)-7-methyl-5-octenoic acid (11 and 10) verified by signal of proton on tertiary carbon δ 2.27-2.18 ppm (m, CH, 1H) ($CDCl_3$)

To achieve (*E/Z*)-7-Methyl-5-octenol (**12** and **13**), reduction of *(E/Z)*-7-methyl-5-octenoic acid (**11** and **10**) was achieved by using $LiAlH_4$ in anh.THF as a reducing agent. Mixture of **11** and **10** was reduced to corresponding mixture of primary alcohols **12** and **13**

The structure of (*E/Z*)-7-Methyl-5-octenol (**12** and **13**), was identified by ^{1}H NMR, found that the chemical shift of CH_2 proton closely OH group at 3.64 ppm (t, *J*=6.6 Hz, 2H) after removed C=O bond (Figure 20).

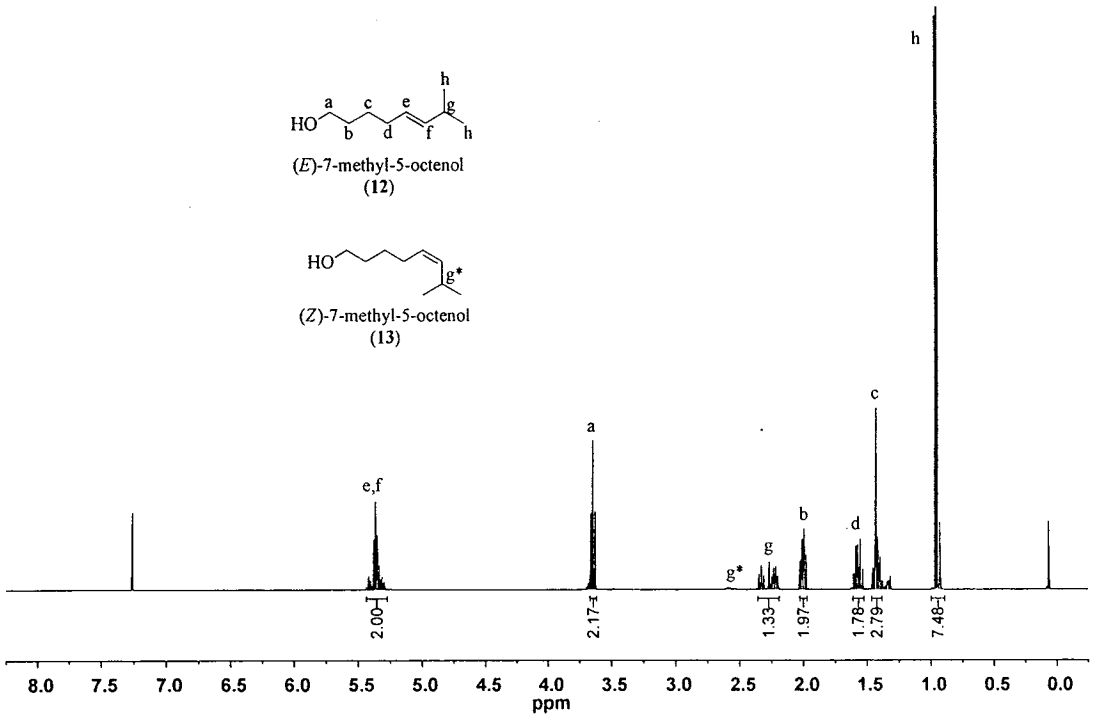

Figure 20 ^{1}H NMR Spectrum of mixture (*E/Z*)- 7-methyl-5-octenol (12 and 13) confirmed signal of proton on CH_2 carbon closely to OH group at δ 3.64 ppm (t, *J*=6.6 Hz, 2H) ($CDCl_3$)

Furthermore, the overlay spectrum ^{1}H NMR were confirmed from compound **10**, **11**, **12** and **13**. The chemical shift of proton on tertiary carbon of **10** was shift from 2.59-2.48 to 2.27-2.18 ppm in consequence of the anisotropic effect and reduction of **11** to **12** and **10** to **13** was shown peak of CH_2 proton closely OH group at 3.64 ppm (*t*, *J*=6.6 Hz, 2H) after reduced C=O bond of carboxylic to primary alcohol (Figure 21) and reconfirmed by FT-IR (KBr) cm^{-1}: 3,361 (O-H stretching), by missing of 1,658 (C=O stretching) (Figure 22).

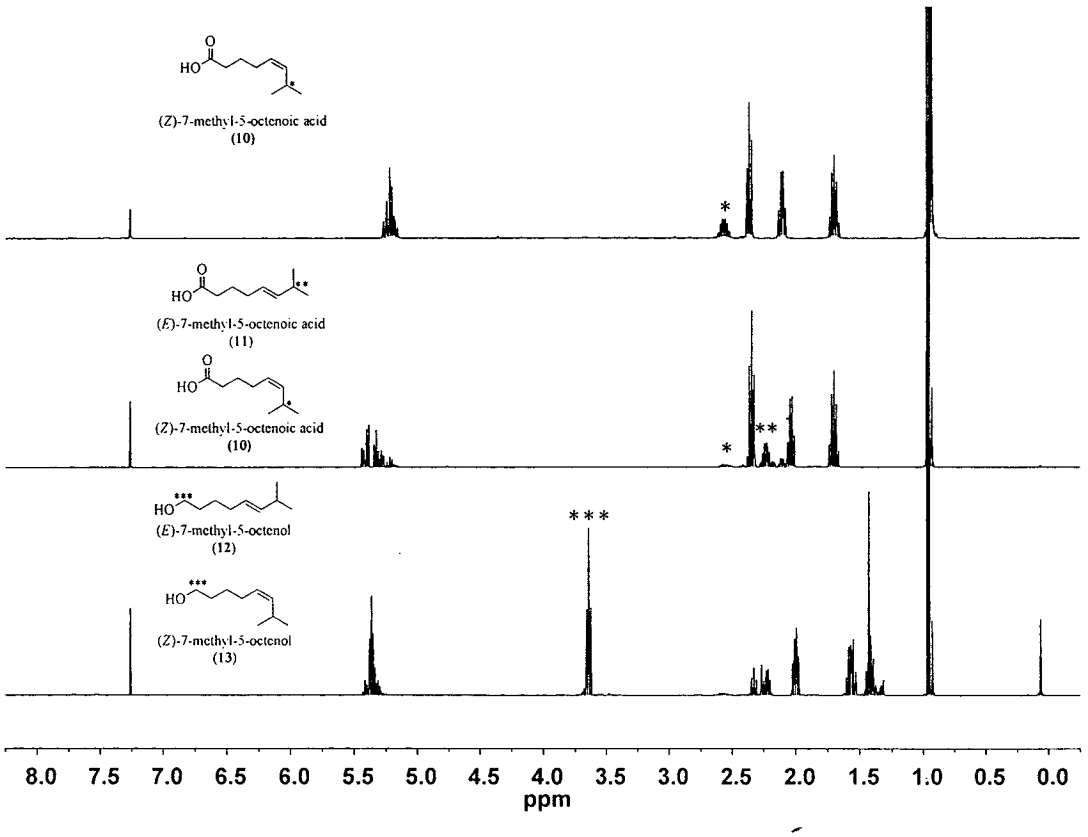

Figure 21 Overlay spectrum of mixture (*E/Z*)- 7-methyl-5-octenol (12 and 13) confirmed signal of proton on CH_2 carbon closely to OH group at δ 3.64 ppm (*t*, *J*=6.6 Hz, 2H) ($CDCl_3$)

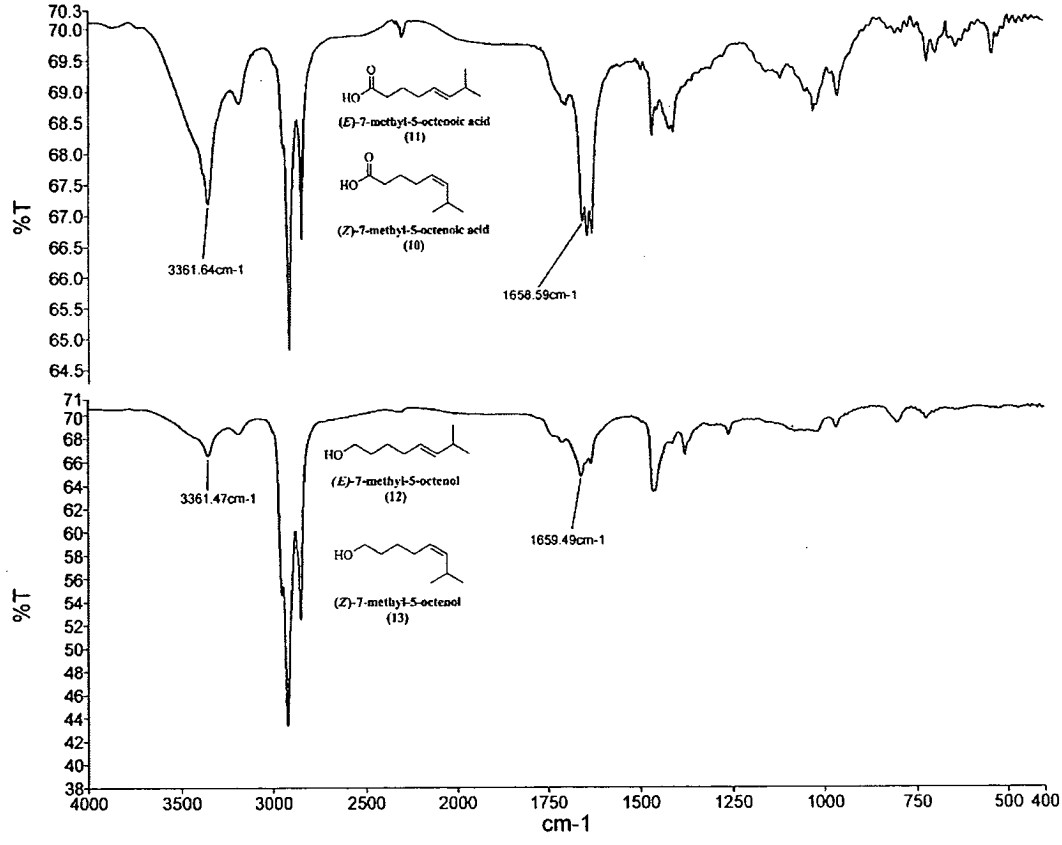

Figure 22 Overlay FT-IR spectrum of mixture *(E/Z)*-7-methyl-5-octenoic acid (11 and 10) and (*E/Z*)-7-Methyl-5-octenol (12 and 13): 3,361 cm^{-1} (O-H stretching), by missing of 1,658 cm^{-1} (C=O stretching)

2. Synthesis of capsinoid analogue 4 and 5

Capsinoid analogue **4** and **5** were synthesized *via* esterification reaction by using DCC, DMAP and HOBt. DMAP, was employed as a strong nucleophile to activated homovanillic acid (**14**) to acetate intermediate. Then, DCC and the acetate intermediate were able to form an *O*-acylisourea intermediate after that lone pair electron of oxygen from HOBt attacked at carbonyl position to afford "active ester" and dicyclohexylurea (DCU) as by-product which easily eliminated *via* recrystallization in hexane and filtration. This step was faster than normal esterification that used only DCC and DMAP. In the presence of DMAP, the alcohol was activated to alkoxide for attacking at carbonyl carbon of "active ester" to cleave hydroxybenzotriazole out as by-product to produce capsinoid analogue (Appendix B).

capsinoid analogue **4** and **5** was obtained 62% yields with ratio of **4** (*E*-isomer) and **5** (*Z*-isomer) at 85:15. The crude product was first purified by column chromatography with 30% EtOAc in Hexane. The structure of **4** and **5** was confirmed by ^{1}H NMR as shown in Figure 23 and the overlay spectrum of homovanillic acid (**14**), *(E/Z)*-7-methyl-5-octenol (**12** and **13**) and capsinoid analogue **4** and **5** were also definitely confirmed.

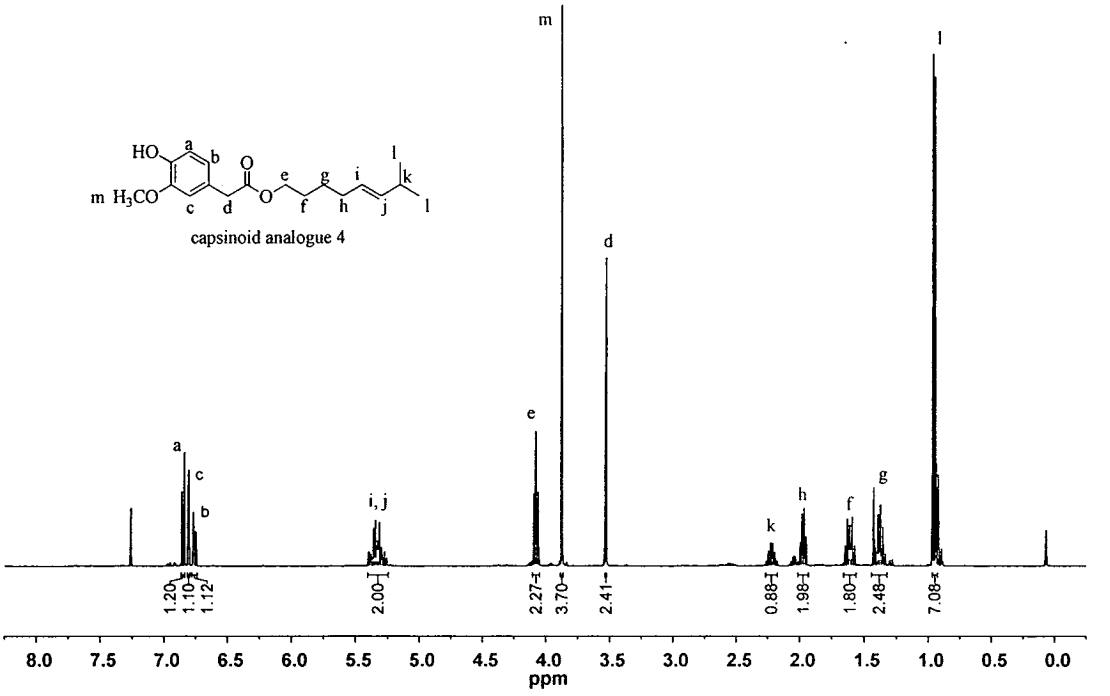

Figure 23 ^{1}H NMR Spectrum of capsinoid analogue 4 ($CDCl_3$)

The overlay spectrum was shown the position of CH_2 closely to OH-group of alcohol **12** and **13** shift from 3.67 to 4.10 when coupling with homovanillic acid to confirm that was CH_2 of ester bond in capsinoid analogue **4** and **5** (Figure 24) and reconfirmed by FT-IR (KBr) 3,447 cm^{-1} of phenol (O-H stretching), 1,735 cm^{-1} (C=O stretching), and 1,035 cm^{-1} C-O stretching of ester bond. (Figure 25)

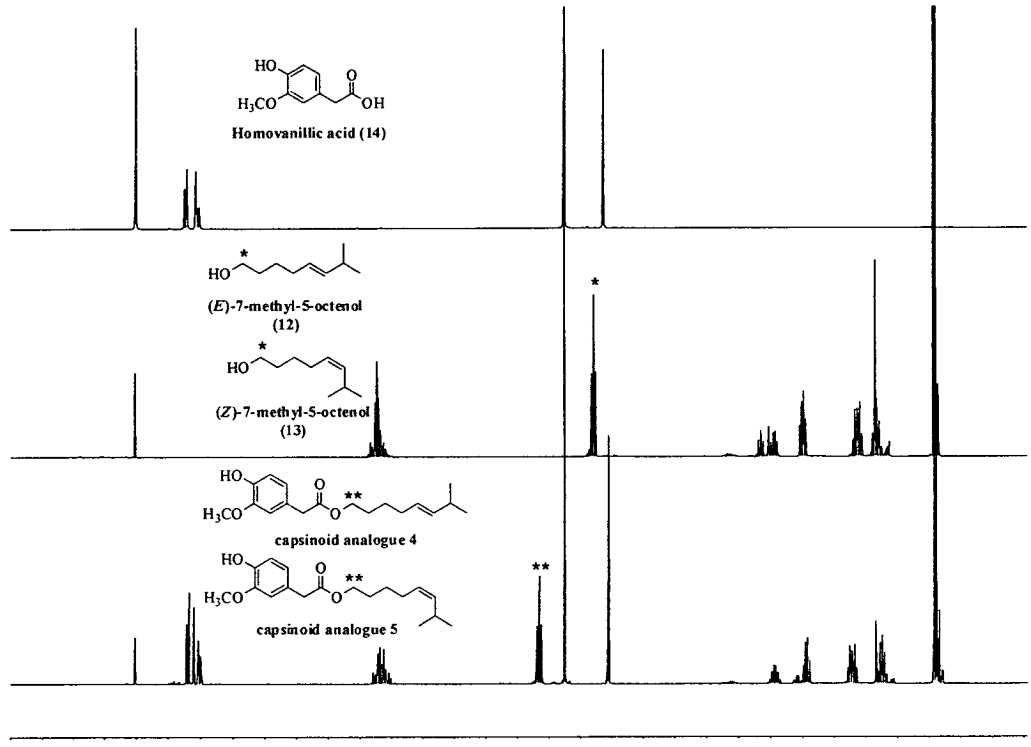

Figure 24 Overlay spectrum of homovanillic acid (14), (*E/Z*)-7-methyl-5-octenol (12 and 13) and capsinoid analogue 4 and 5 ($CDCl_3$)

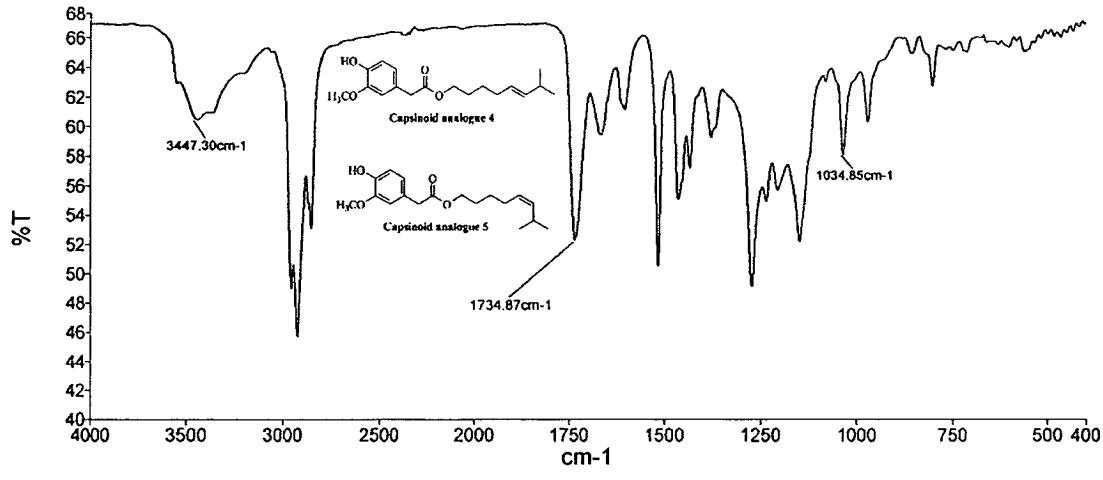

Figure 25 FT-IR spectrum of mixture capsinoid analogue 4 and 5: 3,447 cm^{-1} of phenol (O-H stretching), 1,735 cm^{-1} (C=O stretching), and 1,035 cm^{-1} C-O stretching of ester bond

As a major product, only ^{13}C-NMR, DEPT 90 and DEPT 135 (400 MHz, $CDCl_3$) of capsinoid analogue (4) can be performed and it was firmly identified the structure as shown in Figure 26, DEPT 90 to identified only the chemical shift of CH at 138.42, 126.57, 122.32, 114.52, 111.90, and 31.16, respectively. DEPT 135 to confirm CH_2 signals was shown negative peak at 65.07, 41.26, 31.99, 28.23, and 26.06, respectively while CH and CH_3 were shown positive peak. It was found δ of CH_3 at 56.09, 22.82, and 22.62, respectively. The chemical shift of ^{13}C was shown at 171.95, 146.48, 144.64, and 125.72, respectively.

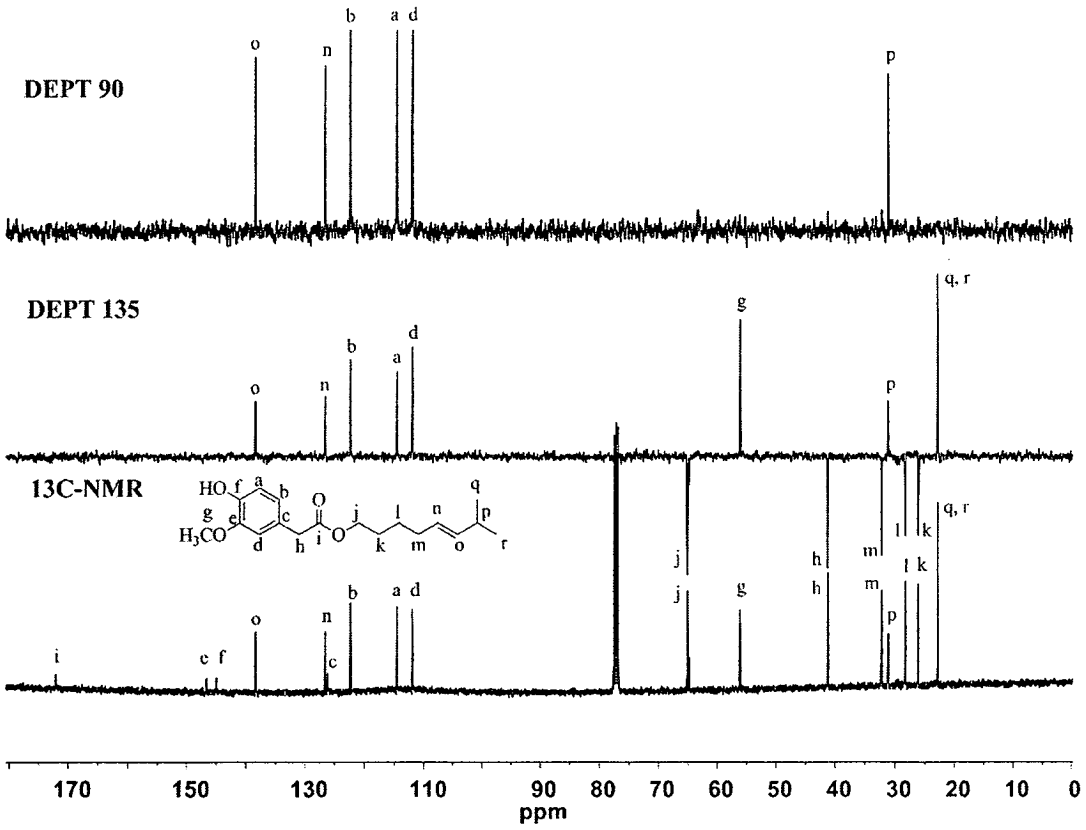

Figure 26 ^{13}C-NMR, DEPT 90 and DEPT 135 of capsinoid analogue 4 (400 MHz, $CDCl_3$)

3. Synthesis of *(E)*-8-methyl-6-nonenol (17) and 8-methylnonanol (18)

To prepare the mixture of (*E*)-8-Methyl-6-nonenol (**17**) and 8-methylnonanol (**18**), reduction of **15** and **16** (isolated and precipitated from crude chili extract following with acid hydrolysis) was performed by using $LiAlH_4$ as a reducing agent.

The overlay spectrum ^{1}H NMR was identified the mixture compounds of **17** and **18** with 95% yields. The reduction was shown peak of CH_2 proton closely OH group at 3.68 ppm (*t*, *J*=6.8 Hz, 4H) (Figure 27) and reconfirmed by FT-IR (KBr) cm^{-1}: 3,369 (O-H stretching), by missing of 1,710 (C=O stretching) (Figure 28).

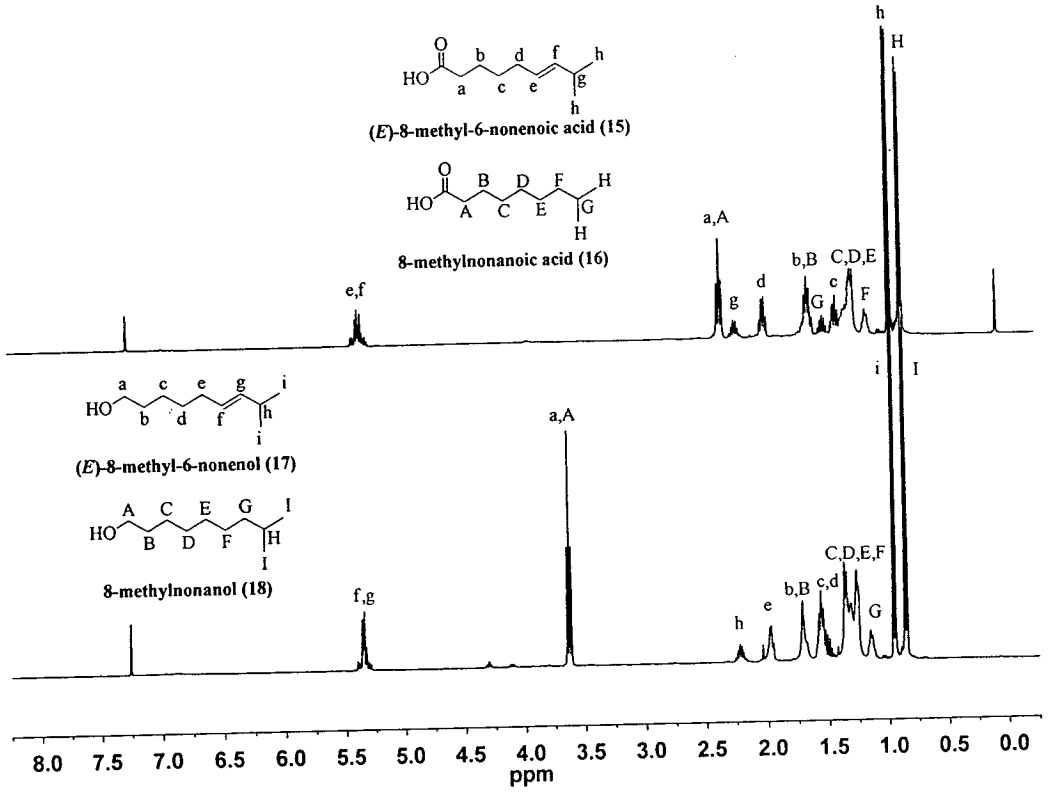

Figure 27 Overlay spectrum the mixture of *(E)*-8-methyl-6-nonenol (17) and 8-methylnonanol (18) confirmed signal of proton on CH_2 carbon closely to OH group at δ 3.68 ppm (t, *J*=6.8 Hz, 4H) ($CDCl_3$)

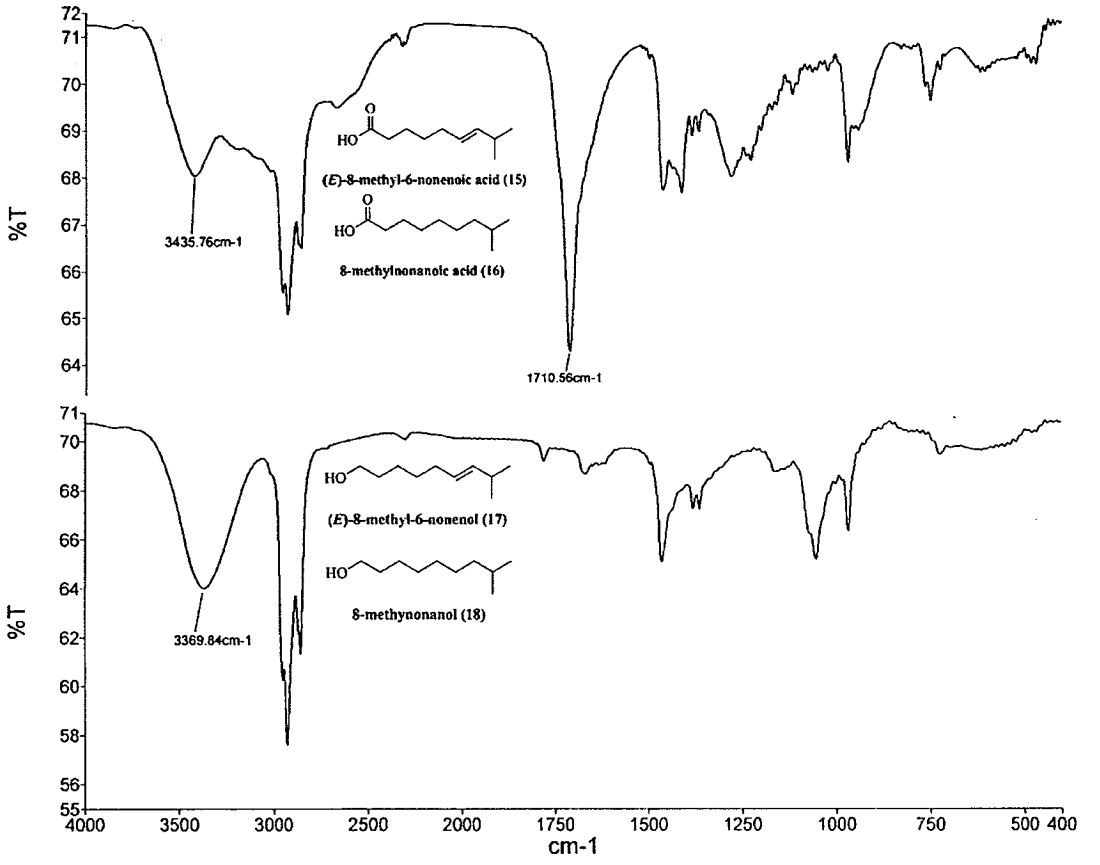

Figure 28 Overlay FT-IR spectrum of mixture *(E)*-8-methyl-6-nonenol (17) and 8-methylnonanol (18) : 3,369 cm^{-1} (O-H stretching), by missing of 1,710 cm^{-1} (C=O stretching).

4. Synthesis the mixture of capsinoid analogue 6 and 7

Similarly to the synthesis of capsinoid analogue **4** and **5** procedure, capsinoid analogue **6** and **7** was accomplished *via* esterification reaction by using DCC, DMAP and HOBt to produce capsinoid analogue **6** and **7**, respectively. Capsinoid analogue **6** and **7** was achieved from esterification reaction with 77% yields with the mixture of *trans* and dihydro capsinoid analogue. The crude product was first purified by column chromatography 30% EtOAc in Hexane. The structure of capsinoids analogue **6** and **7** were confirmed by ^1H NMR as shown in Figure 29 and the overlay spectrum of homovanillic acid (**14**), *(E)*-8-methyl-6-nonenol (**17**) and 8-methylnonanol (**18**) and capsinoids analogues **6** and **7** were also definitely confirmed in Figure 30. The overlay spectrum was shown the position of CH_2 closely to OH-

group of alcohol **17** and **18** shift from 3.68 to 4.12 when coupling with homovanillic acid (**14**) to confirm that was CH_2 of ester bond in capsinoid analogue **6** and **7**, and reconfirmed by FT-IR (KBr) 3,446 cm^{-1} of phenol (O-H stretching), 1,734 cm^{-1} (C=O stretching), and 1,033 cm^{-1} C-O stretching of ester bond. (Figure 31).

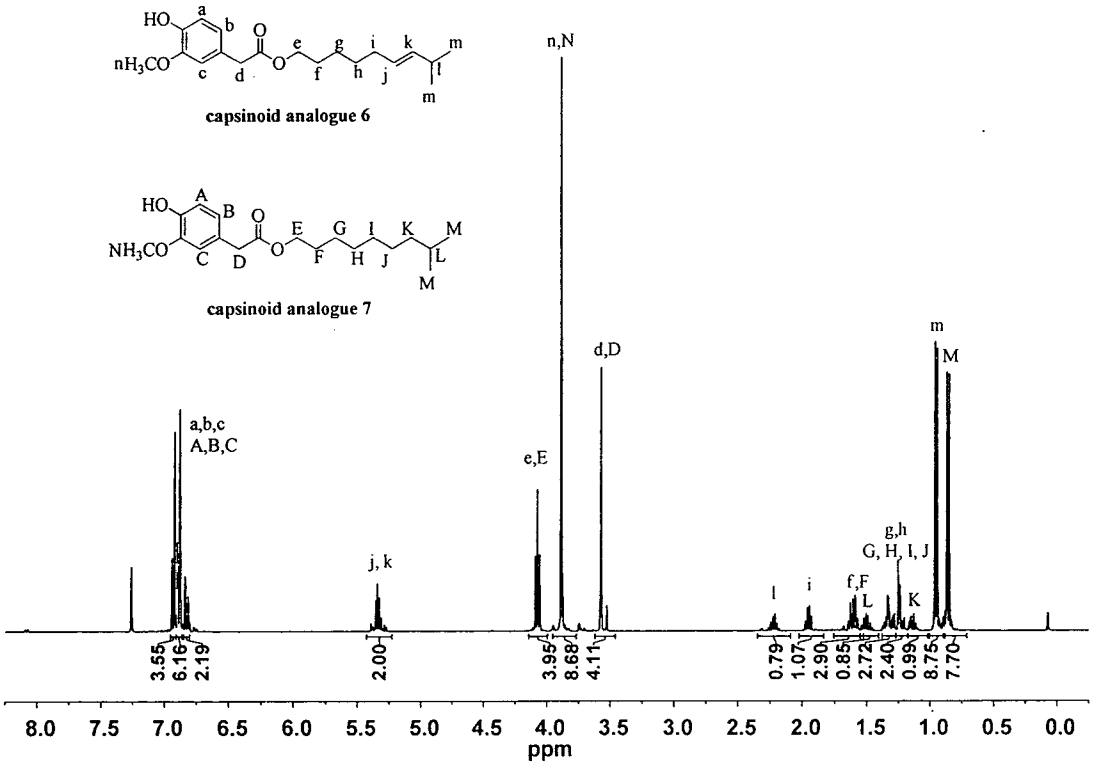

Figure 29 ^{1}H NMR Spectrum of capsinoid analogue 6 and 7, ($CDCl_3$)

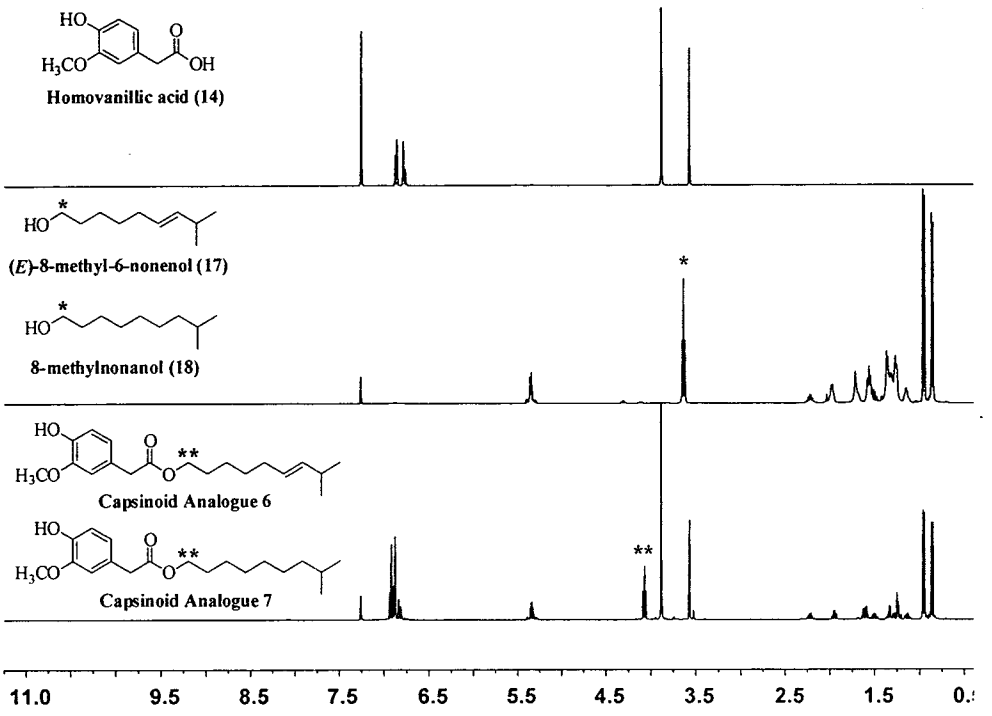

Figure 30 Overlay spectrum of homovanillic acid (14), *(E)*-8-methyl-6-nonenol (17) and 8-methylnonanol (18) and capsinoid analogue 6 and 7 ($CDCl_3$)

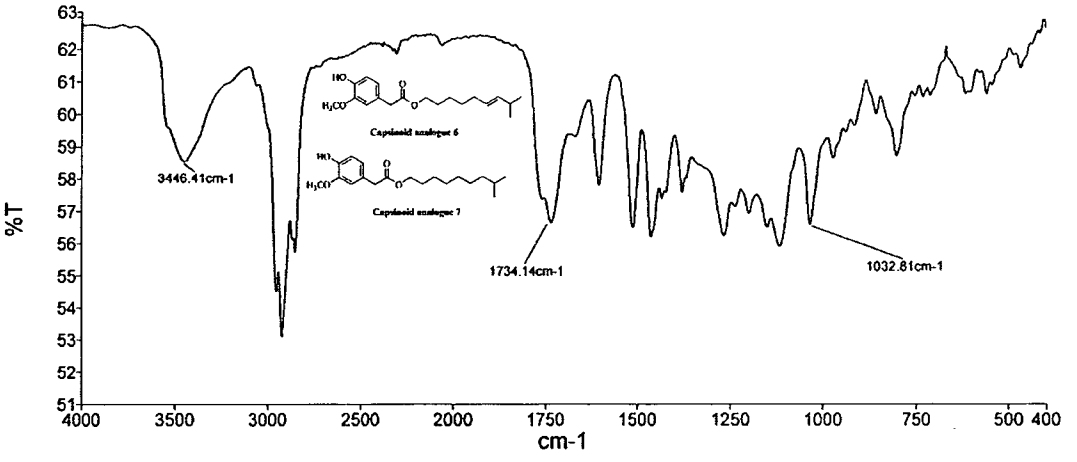

Figure 31 FT-IR spectrum of mixture capsinoid analogue 6 and 7: 3,446 cm^{-1} of phenol (O-H stretching), 1,734 cm^{-1} (C=O stretching), and 1,033 cm^{-1} C-O stretching of ester bond

Stability of capsinoid analogues (4-7) in polar protic solvent

To investigate stability of capsinoid analogues (**4-7**) compare with capsiate, the solubility and the stability in cell solution (buffer pH 7.4) was required. With highly lipophilicity of capsiate and capsinoid analogues, the stability test in cell solution was not probably monitored. Consequently, the solvent system which used under this investigation must be adjusted for capsiate and capsinoid analogues can be dissolved while maintaining the polarity and protic property comparable to cell solution and it was found that the most appropriate system to use as a polar protic solvent was 80 % methanol in water. Additionally, it can be dissolved capsiate and capsinoid analogues as well as provide a well separated (*E*) and (*Z*) isomer peak in HPLC chromtogram. Moreover, 0.025 % of acetic acid was also employed to increase the efficiency of isomer separation, chromatogram of capsinoid analogues (**4-7**) as shown in Figure 32. Chromatogram shown retention time of capsinoid analogue **4** and capsinoid analogue **5** at 29.56 and 28.47 min, respectively, capsinoid analogue **6** was presented at 50.80 and capsinoid analogue **7** at 73.13 min, respectively.

During the stability study, capsinoid analogue **4** and capsinoid analogue **5**, capsinoid analogue **6**, and capsinoid analogue **7** were observed for every 6 hours and percent remaining compared with *E/Z*-capsiate as shown in Figure 33. The results showed that in 24 hours, the remaining percent of *E*-capsiate and *Z*-capsiate were 86% and 59%, respectively. Interestingly, *Z*-capsiate was degraded faster than *E*-capsiate. However, all of capsinoid analogues (**4-7**), were still show no sign of decomposition throughout period of 24 hours. Clearly, they showed that they were highly stable than both *E/Z* capsiate. (Table 5)

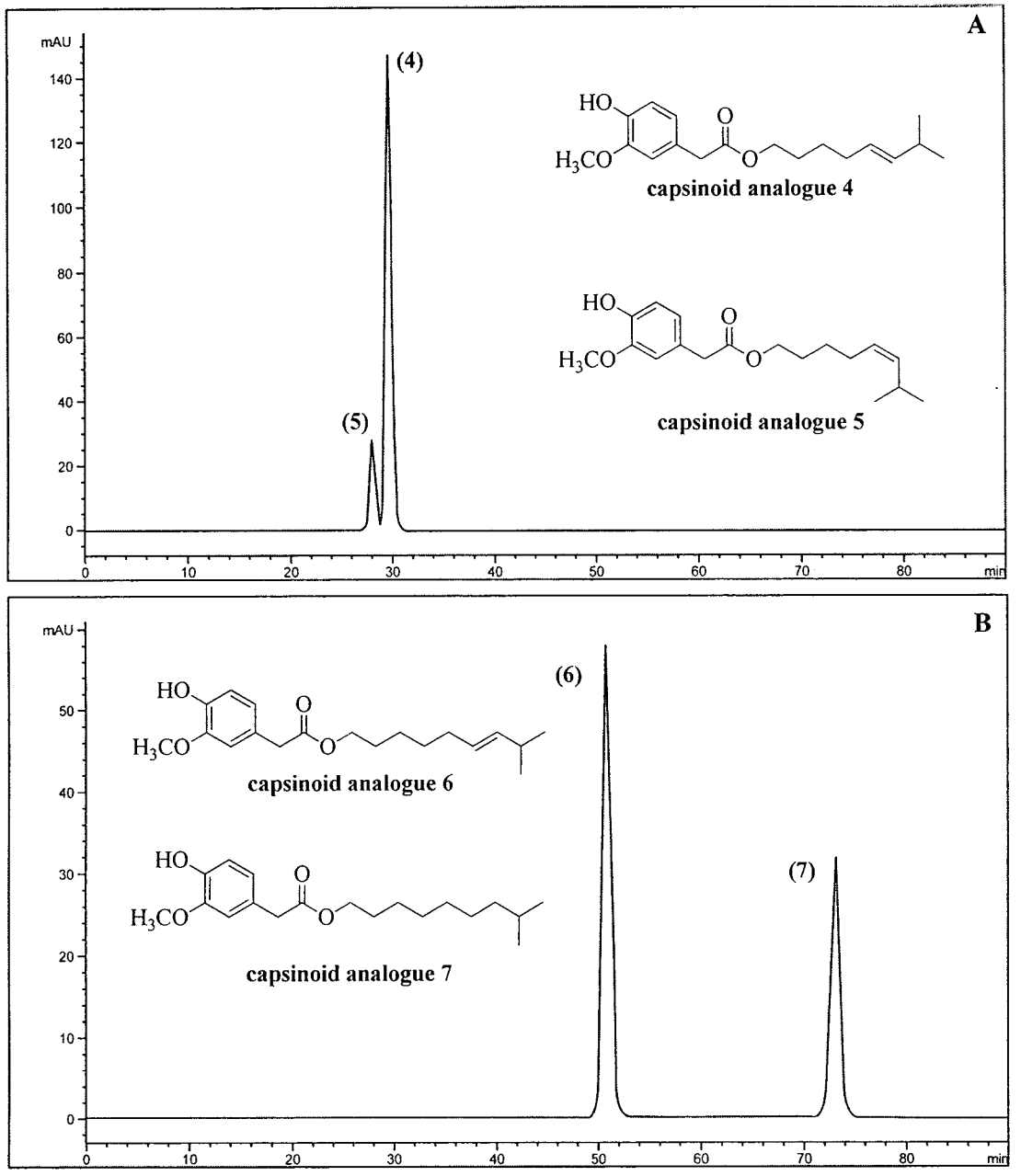

Figure 32 Chromatogram of capsinoid analogues (4-7), at 0 hour, C18, 4.6 x 250 mm, 5 μm, mobile phase, CH_3OH:H_2O/80:20 v/v with 0.025 AcOH, flow rate 0.5 mL/min, detection UV 280 nm; (A) capsinoid analogues 4 and 5 (B) capsinoid analogue 6 and 7

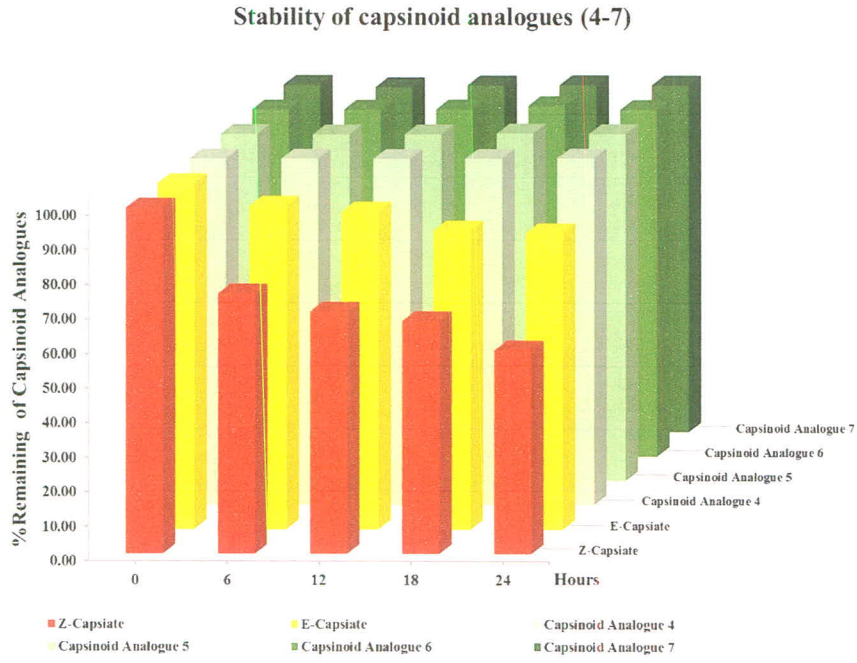

Figure 33 Percent remaining of capsinoid analogues (4-7) within 24 hours. The instance area were observed every 6 hours.

Table 5 Percent remaining of capsinoid analogues (4-7) compared with *E/Z*-capsiate (N = 4)

Hour	% Remaining of Capsinoid Analogues				% Remaining of control	
	Capsinoid Analogue (4)	Capsinoid Analogue (5)	Capsinoid Analogue (6)	Capsinoid Analogue (7)	*E*-Capsiate	*Z*-Capsiate
0	100.00 ± 0.00	100.00 ± 0.00	100.00 ± 0.00	100.00 ± 0.00	100.00 ± 0.00	100.00 ± 0.00
6	100.02 ± 0.02	99.94 ± 0.09	100.02 ± 0.12	99.36 ± 0.47	93.49 ± 2.08	75.27 ± 2.18
12	100.01 ± 0.03	100.00 ± 0.05	100.08 ± 0.06	99.96 ± 0.04	91.84 ± 2.12	70.01 ± 1.06
18	100.08 ± 0.12	100.29 ± 0.59	101.12 ± 0.24	100.03 ± 0.04	86.43 ± 2.24	67.32 ± 2.64
24	100.21 ± 0.07	100.16 ± 0.08	100.05 ± 0.03	100.00 ± 0.02	85.70 ± 0.56	58.90 ± 0.17

The unstable of capsinoids was contributed from stabilization of electron donating group at vanilliod residue (OH-group) to the benzylic carbocation that connected to the ester linkage. If the benzylic carbocation can be stabilized very well from any strong electron donating groups, it will create capsinoids become even

highly unstable regardless of what type of fatty acid connected to capsinoid structure. This instability mechanism was previously discussed by research group from Ajinomoto [31]. Clearly, the position of electron donating group substituents was the crucial factor under this degradation process.

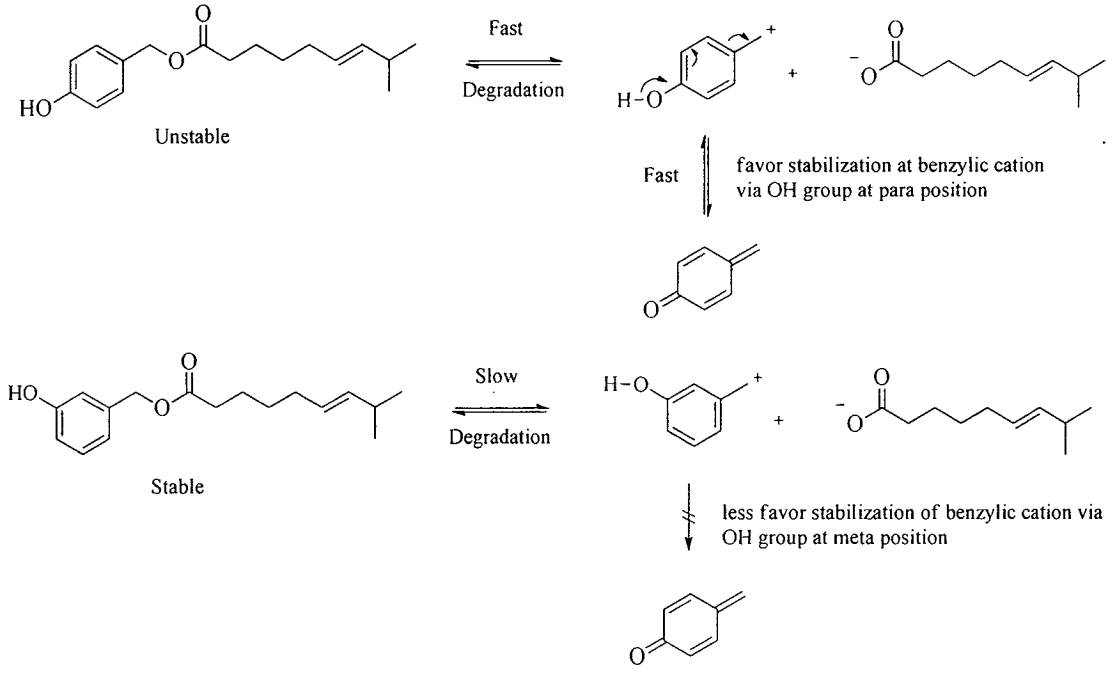

Scheme 18 Degradation mechanism of conventional capsinoids in protic solvent

With the new structural design in order to extent or prolong shelf life of caspsiniod analogues under this investigation, we proposed to inversed the position of ester linkage due to the recognition that *p*-quinonemethide degradation was required at least the leaving group in order to undergo degradation. Therefore, the better of the leaving groups are, the faster of degradation process; consequently, instability of capsinoids. In the contrast, if the vanilloid residue is connected to a very poor leaving group, the cleavage between benzylic carbon and ester group will be less favor resulting higher stability of capsinoids

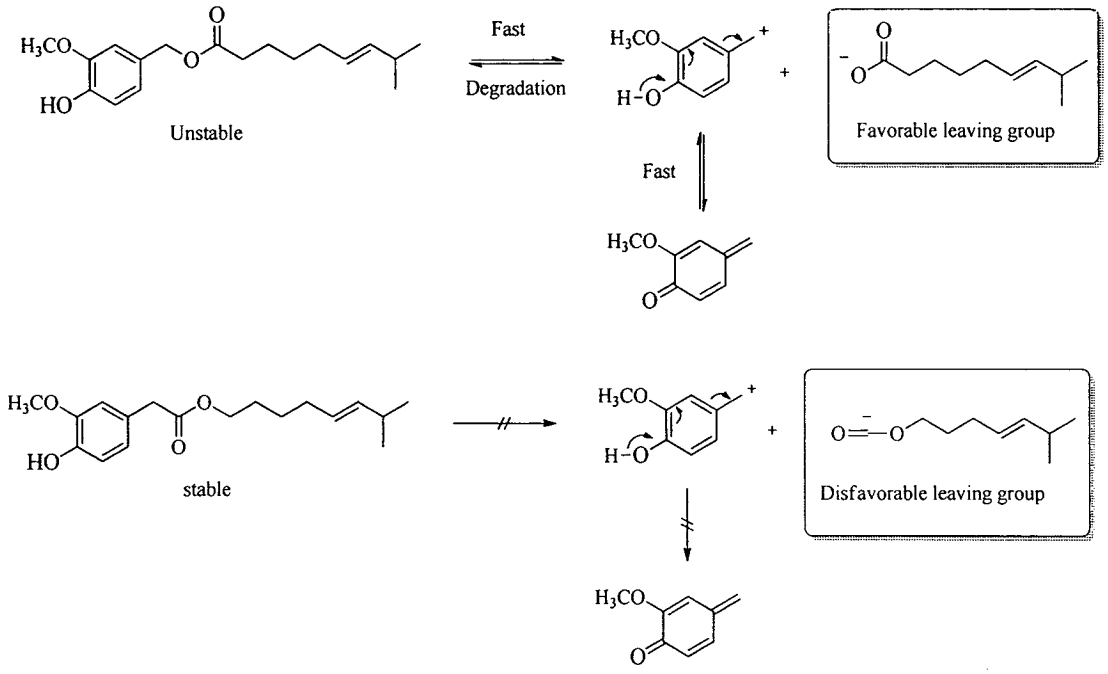

Scheme 19 Proposed stability of inversed ester position in capsinoid analogues in protic solvent compared with conventional *E*-capsiate

To prove our concept, the conventional capsinoids and the inversed capsinoid analogues were dissolved in protic solvent system to observe the remaining of starting products. As expected, *E*-capsiate was constantly degraded over a period of 24 hours while the inversed capsinoid analogue **4** was highly stable over a period of 24 hours. This might due to the leaving group of *E*-capsiate is carboxylate anion which is a better leaving group than acylium anion in inversed capsinoid analogue **4**. This experiment was at least proved the concept of stabilization of leaving group. More of stabilization process needs to be explored in order to full understand the other effect such as effect of electron withdrawing group.

Investigation of cell viability on Caco-2 cell and cytotoxicity *via* MTT assays

To evaluate the cell viability and cytotoxicity of capsinoid analogues (**4-7**), a preliminary screening was performed in Caco-2 cells, a human colorectal adenocarcinoma cell line isolated from colon carcinoma tissue and generally used as in *vitro* models of intestinal drug absorption, using MTT (3-(4,5-Dimethylthiazol-2-yl)-2,5-diphenyltetrazolium bromide) assay to measure numbers of viable cells as living cells. This is because MTT is specifically reduced by mitochondrial reductase only in

active mitochondria; consequently, tetrazolium ring of MTT is rapidly cleaved to produce formazan dye which has a purple color. (Scheme 20) It was suggested that MTT was up take by cells through endocytosis and the formazan gradually accumulated in the endosomal/lysosomal compartment and was then transported to the cell surface through exocytosis. [41]

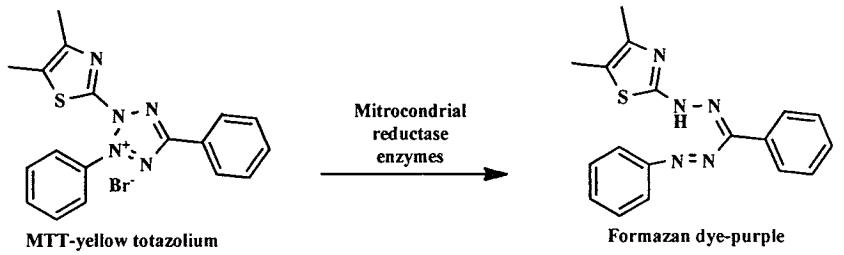

Scheme 20 Mechanism of MTT inside active mitochondria [42]

Experimentally, Caco-2 cells were cultured and treated with capsinoid analogues (**4-7**) and capsaicin was used as negative control while capsiate was used as positive control. The concentration dose of capsinoid analogues (**4-7**) were ranged from 0.1, 1.0, 10.0, 100.0, and 200.0 μM, respectively in 1% PEG+DMEM vehicle for 18 and 24 hours incubation periods.

The results showed that capsaicin induced significantly reduction of viable cells in a dose- and time-dependent manner, as shown in Figure 34 and 35. Incubation with capsaicin at the highest dose, 200 μM, for 18 hours considerably decreased the number of cell viability approximately up to 50% compared to the control. At the maximum concentrations of capsiate, the number of cells viability was 76% and capsinoid analogues (**4-7**) were 83%, 84%, 90% and 97%, respectively. As the results of 24 hours, at the maximum dose of 200 μM treatment, cell viability of capsaicin was only 47% compared to vehicle while capsiate was 76%. As expected, cell viability of capsinoid analogues (**4-7**) were 81%, 73%, 71% and 75%, respectively. Convincingly, capsinoid analogues (**4-7**) showed no toxicity to Caco-2 cells as similar as capsiate. From this preliminary information, it provided the promising data for further investigation for other biological activities testing as well as anti-obesity testing in the future.

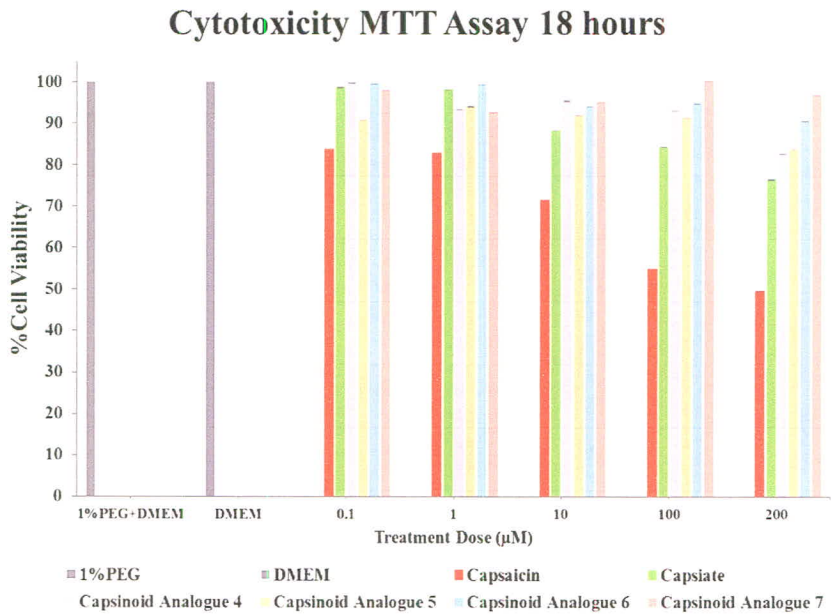

Figure 34 %cell viability of Caco-2 cells by using Cytotoxicity MTT assay treated with capsinoid analogues (4-7), capsaicin use as negative control while capsiate use as positive control and the variation of dose at 0.1, 1.0, 10.0, 100.0, and 200.0 µM, respectively with 1% PEG+DMEM vehicle for 18 hours

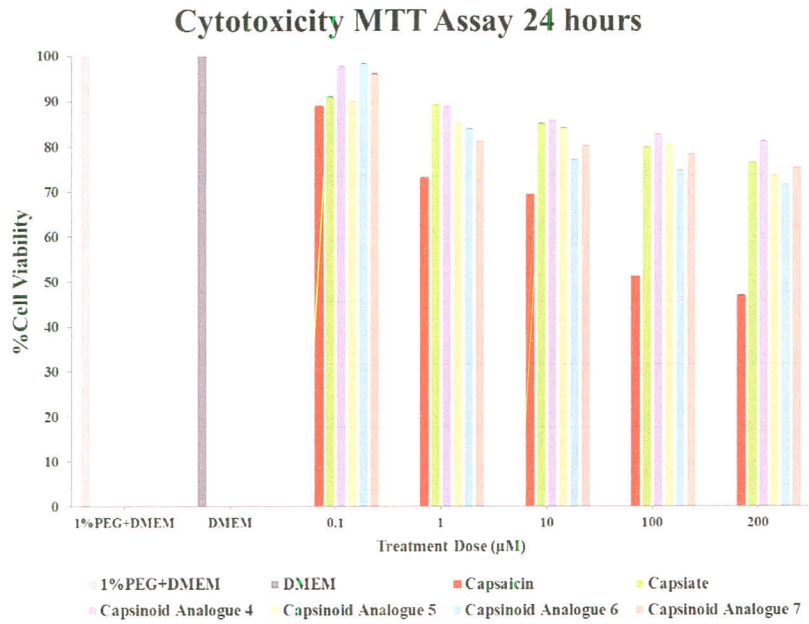

Figure 35 %cell viability of Caco-2 cells by using Cytotoxicity MTT assay treated with capsinoid analogues (4-7), capsaicin use as negative control while capsiate use as positive control and the variation of dose at 0.1, 1.0, 10.0, 100.0, and 200.0 µM, respectively with 1% PEG+DMEM vehicle for 24 hours

Furthermore, IC_{50} value of capsinoid analogues (**4-7**) was examined to investigate the effective concentration dose which was required for 50% inhibition in *vitro*. The variation of concentration dose was 0.1, 1.0, 10.0, 50.0, 100.0, 150.0, and 200.0 µM for cytotoxicity MTT assay and it was measured with spectrometer microplate reader at 595 nm for constructing a dose-response curve and examining the effect of different concentrations of inhibition. IC_{50} values can be calculated by determining the concentration needed to inhibit half of the maximum biological response of the activities. IC_{50} values are very dependent on conditions under which they are measured. In this observation the maximum dose was 200 µM, it was found that IC_{50} value of capsinoid analogues (**4-7**) did not show any cytotoxicity within experimentally used concentration from 200-0.1 µM as IC_{50} values was found beyond the limits. (Figure 36)

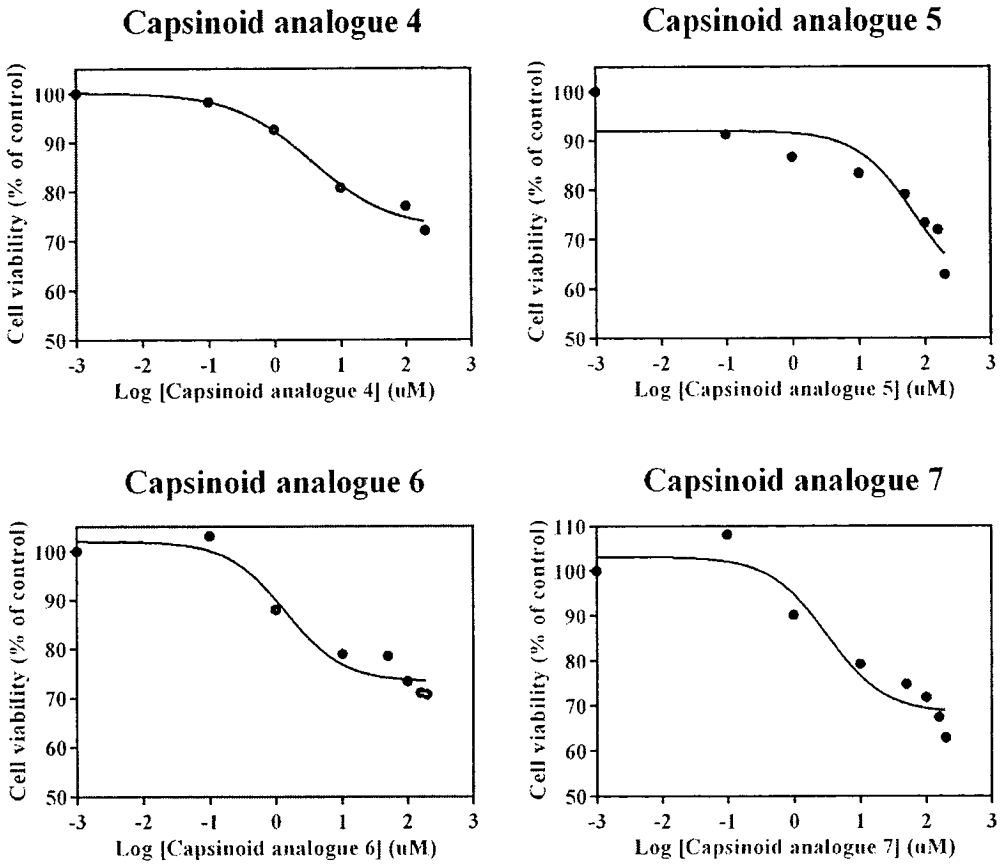

Figure 36 IC_{50} value plot between %Cell viability of control and Log concentration of each analogue (4-7)